Interreg

2 Seas Mers Zeeën

EUROPEAN UNION

European Regional Development Fund

Report No.	**D1.x.x**	
Title of Report:	**Accelerated ageing through electrochemical corrosion**	

Written by: Pankaj Jaiswal (UGent)	Verified by : Wim De Waele (UGent) Luc Mouton (BV) Prakash Venkatesan (TUDelft)	Revision 02	Date 21/09/2020

Contents

List of figures

EXECUTIVE SUMMARY

The interfacial corrosion in a bi-material adhesively bonded joint (CFRP composite plates and steel substrates) could potentially have an adverse effect on the joint's durability. This report focuses on a methodology to study the effect of accelerated ageing on the durability of a double lap adhesive joint (DLAJ) using electrochemical corrosion. The preliminary experimental setup includes a pre-fabricated DLAJ, a stainless steel rod and artificial seawater (ASTM-D1141-98) serving as anode, cathode and electrolyte solution respectively. A representative service life of 5-years was targeted by measuring corrosion activity during 24 hours. Following, a three-anode setup was developed to compare its performance with a single anode setup. The initial results show that the single anode corrosion method (SACM) was relatively more consistent, efficient and accurate than the three-anode corrosion method (TACM). The analytical relation proposed by Faraday allows to predict the deterioration level of steel substrates subjected to accelerated corrosion.

1. Introduction

The quantification of the effects of corrosion on the degradation of the structural integrity of a double lap adhesive joint (DLAJ) exposed to salt water, sea water or tap water using conventional experimental methods can be a time-consuming task. Therefore, the goal of this work was to develop a methodology to accelerate the corrosion process under controlled conditions. A two-electrode electrochemical corrosion methodology was chosen; it comprises a working electrode (anode: test specimen) and a counter electrode (cathode: steel bar) as illustrated in Figure 1. Preliminary tests were performed with a steel plate (grade S235) measuring 300 x 25 x 6 mm^3 (anode) and a steel rod (grade S235) measuring Ø25mm x 300 mm as a cathode. After a pre-determined electrochemical processing time was obtained, the samples were recovered from the setup and weighed (without cleaning corrosion product) after drying with a hairdryer. To prevent residual soft corrosion on the sample, low velocity of hot air from the dryer was maintained for 15 minutes. Then the theoretical and experimental mass loss was compared.

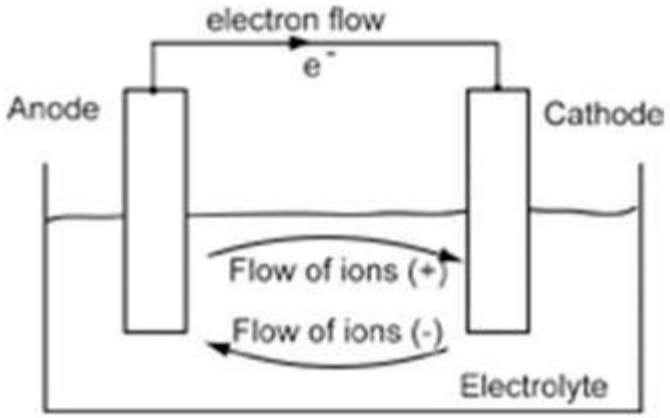

Figure 1 Schematic illustration of electrochemical corrosion cell setup

2. Validation of mass loss

The theoretical mass loss can be directly calculated using Faraday's law of electrolysis [1], [2]:

$$m = \frac{Ita}{nF}$$

where m is the mass loss due to corrosion or the mass of oxidized metal, I is applied electrical current (0.150 ampere), t is the time of electrochemical reaction (86400 seconds), a is the atomic weight of corroding metal (55.9 gram/mol), n is the amount of electrons transferred in the oxidation reaction (mole) or the number of electrons or ionic charge (n = 2 for Fe^{2+}) and F is Faraday's constant (96500 coulombs/equivalent).

This mathematical equation yields a theoretical mass loss of 3.761 grams of steel after 24 hours of exposure. In order to validate the theoretical mass loss, the first trial was performed using a steel specimen in a single anode configuration, called a single anode corrosion method (SACM). A direct current (DC) was applied using a bench potentiostat (allowing current intensities ranging between 0 to 5 amperes). A fixed current of 150 mA was applied based on literature [3]. The steel plate specimen was submerged over a length of 156 mm in a six-liters artificial salt water solution (5% sodium chloride (NaCl)) in a plastic container. The lab setup for the single anode corrosion method can be seen in Figure 2.

Following, a setup was build that allows performing electrochemical corrosion tests on multiple specimens simultaneously. A triple anode configuration, called triple anode corrosion method (TACM), consists of three anode steel plates placed equidistant from the cathode (Figure 3). During this process,

the applied electrical current was increased proportionally from 150 mA to 450 mA in order to obtain a similar mass loss as in the single anode setup.

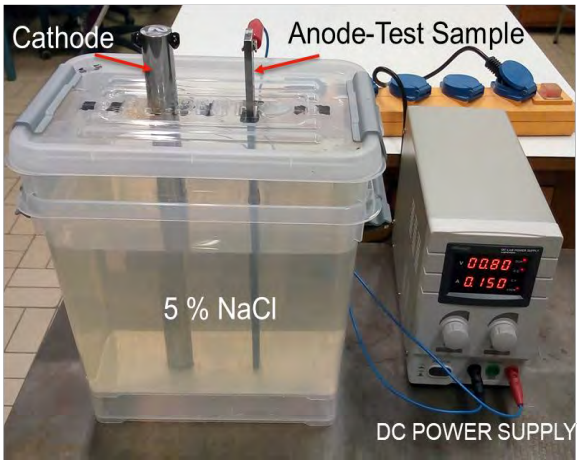

Figure 2 : A single anode corrosion cell setup (SACM)

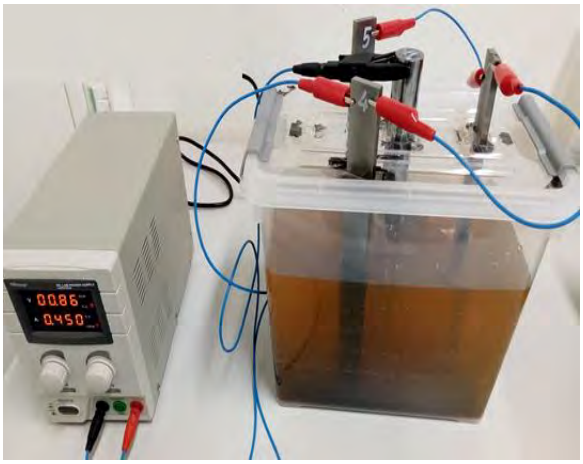

Figure 3 : The triple anode corrosion cell setup (TACM)

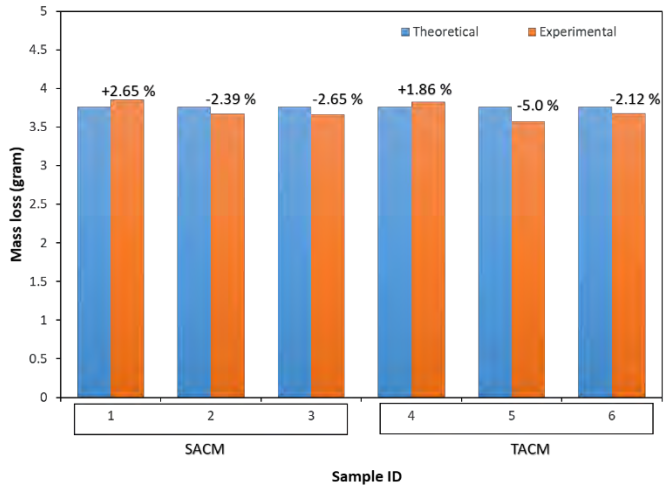

Figure 4 Theoretical and experimental mass loss for SACM and TACM.

Figure 5 The degraded steel samples after TACM

Table 1 Summary of the preliminary test results

Sample ID	Duration of exposure (Hours)	Type of corrosion method	Current intensity (Amperes)	Theoretical (Predicted) mass loss (Grams)	Experimental mass loss (Grams)	Exposed area (cm^2)
01	24	SACM	0.150	3.76	3.86	37.5
02					3.67	
03					3.66	
04		TACM	0.450	34.6	3.83	37.5
05				34.6	3.57	
06				34.6	3.68	

In total, six samples have been exposed to electrochemical corrosion for 24 hours. Three specimens were tested using the SACM and three specimens with TACM at an ambient temperature of 20 ±2 °C and an environmental humidity of 45±2 %. Figure 4 shows the predicted (theoretical) mass loss compared to the experimental mass loss for both corrosion methods. The experimental mass loss measured by SACM was on average closer to the theoretical mass loss, although the differences with the TACM results are not very significant. The observed variation in mismatch between theoretically calculated and experimentally measured mass losses is most probably due to the lack of an established protocol for sample cleaning. Based on the results of the TACM setup, it was observed that there was indeed a linear proportionality between the electric current and mass loss, as stated by the first law of Faraday. Figure 5 shows the state of the specimens after the electrochemical corrosion.
Table *1* summarizes the predicted and experimentally achieved mass losses for each sample.

3. Tafel experiment

The purpose of this experiment is to evaluate the corrosion rate and to determine the corrosion current density of the electrode material under natural/free corroding conditions. In this experiment, a three-electrode configuration was used instead of a two-electrode configuration. In a two-electrode configuration, an appropriate potential is applied between the electrodes to induce corrosion, where the absolute potential of either of the electrodes is unknown. The drawback of this configuration is that it cannot provide information regarding the electrochemical performance of the individual electrodes; however, it gives useful insights into the performance of the entire electrochemical system. On the other hand, the three-electrode system consists of a working electrode (the sample), a reference electrode and a counter electrode.. The three-electrode electrochemical measurement system consisted of artificial seawater (as per ASTM D 1141 – 98 [4]) as an electrolyte, Ag/AgCl saturated in 3M KCl solution as a reference electrode and a Platinum–Rhodium (10 wt%) wire of 0.07 mm diameter as a counter electrode. The Vertex potentiostat from Ivium Technologies was used; it has a current range of ± 1 A and potential range of ± 10 V. Further specifications of the potentiostat are given in Table 2.

Table 2 Specifications of the potentiostat

Instrument	Vertex from Ivium Technologies
Current compliance	±1 A
Current range	10 nA to 1 A
Maximum output voltage	±10 V
Data acquisition rate	100 kHz

The electrochemical measurements were done to determine the corrosion potential (Ecorr) of the steel material used in the bi-material adhesive joints. The corrosion potential was determined in three steps. First a polarization curve, i.e. the profile of applied potential versus measured current, was determined by applying a range of potential (±250 mV) with respect to the Open Circuit Potential (OCP) at a sweep rate of 1 mV/s. Second, a Tafel curve was obtained from the polarization curve by plotting the applied potential versus logarithm of electrical current. Such Tafel curve consists of two parts, i.e., anodic and cathodic polarization curves. The third step was to determine the point of intersection of the slopes of the anodic and cathodic polarization curves. The coordinates of the intersection point represent the corrosion potential E_{corr} and the corrosion current density i_{corr}. To eliminate the effect of the relative size of the electrodes, the current density i_{corr} (A/cm^2) was used as the true indication of the corrosion rate. Additionally, the slopes of the anodic and cathodic polarization curves were referred to as Tafel constants.

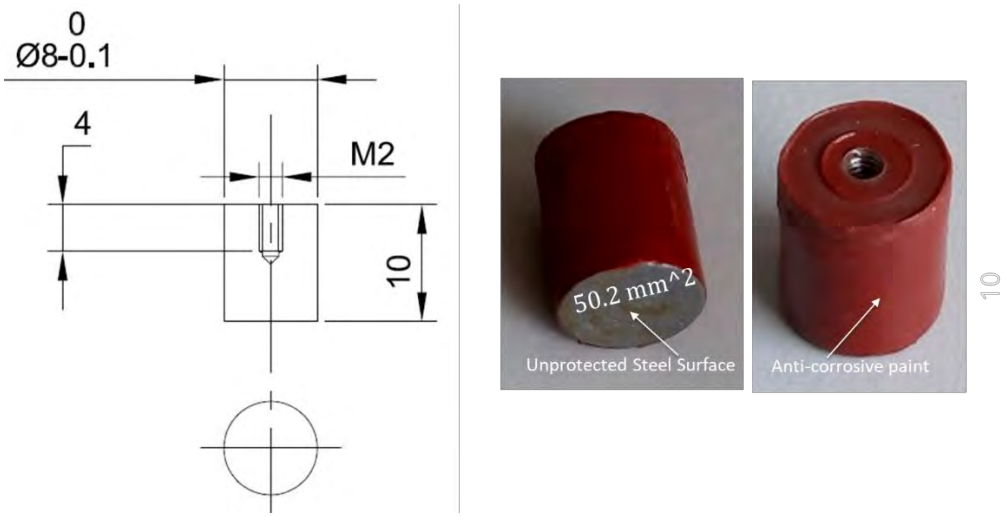

Figure 6 Schematic diagram and final appearance of working electrode (specimen).

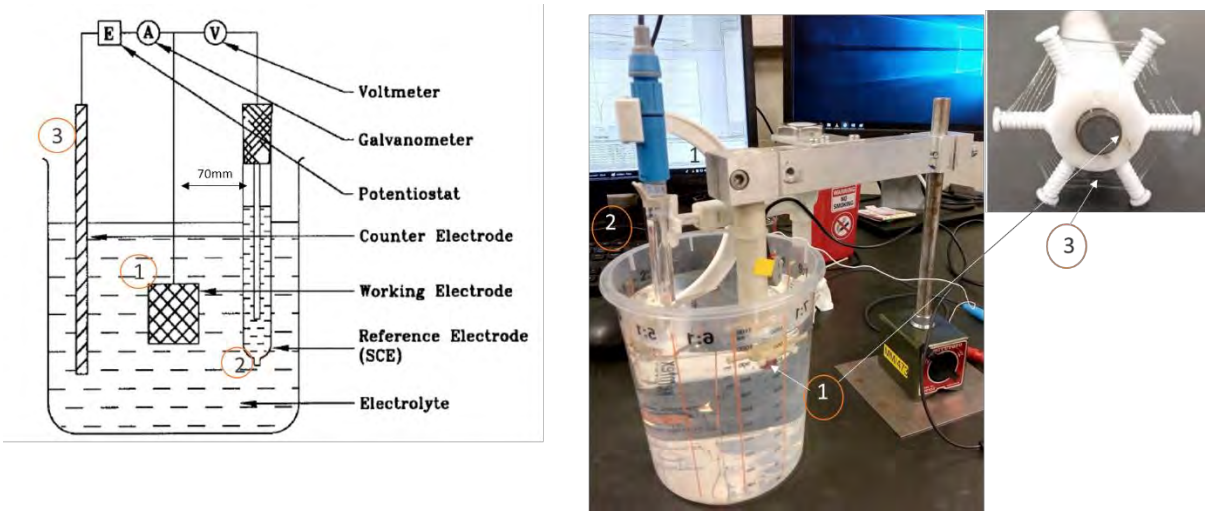

Figure 7 Schematic diagram and laboratory setup for Tafel experiment.

For the Tafel experiments, conventional S235 carbon steel was used for the manufacturing of six working electrodes. The geometrical dimensions and final appearance of the specimens are shown in Figure 6. The three electrodes (working, reference and counter) were placed in a plastic container filled with one liter of electrolyte solution (artificial seawater). The reference and working electrodes were placed as close as possible to each other (i.e. within 70mm) to prevent any possible potential drop. The change in electrical current between the counter and the working electrodes creates different potentials between the reference and the working electrodes. A polarization plot was obtained by scanning at a few values of potential below and above the free corrosion potential. Each plot will have two branches, one corresponding to the cathodic polarization (below Ecorr) and the other to the anodic polarization (above Ecorr). The point of intersection is drawn by taking the slopes of the anodic and cathodic polarization curves. The coordinates of the intersection point represent the corrosion potential, Ecorr and corrosion current density, icorr. The schematic diagram and laboratory setup of Tafel experiment are shown in Figure 7.

3.1 Tafel plots

Figure 8 gives the Tafel curve, showing the current density (log-scale) as a function of the applied potential for sample 01. As mentioned higher, the Tafel curve combines the anodic and cathodic polarization curves. In the anodic region, the specimen surface oxidizes and is thus undergoing corrosion

due to the loss of electrons, whereas in the cathodic region the specimen surface does not undergo oxidation. E_{corr} and i_{corr} are defined at the intersection of the anodic and cathodic type of reactions.

Table 3 Corrosion current density of working electrode (S235 Steel).

Sample Id	Corrosion current density (µA/cm2)	Mean of corrosion current density (µA/cm2)
Sample-01	12.73	
Sample-02	11.37	
Sample-03	13.50	**12.60**
Sample-04	12.67	
Sample-05	12.76	
Sample-06	21.96	

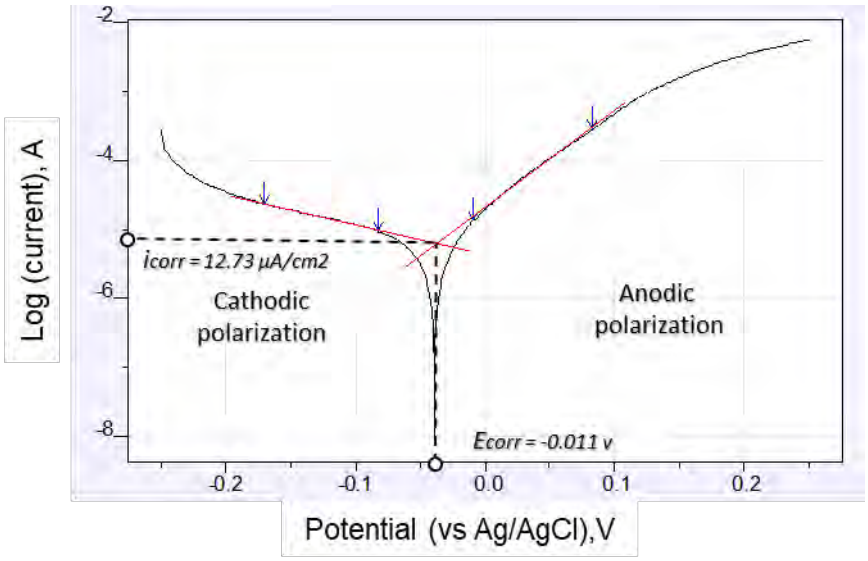

Figure 8 Tafel curve of S235c steel in artificial sea water. Ecorr is obtained at −0.0113 V (vs Ag/AgCl) and the calculated icorr is 12.73 μ A/cm2 i.e., antilog10(-4.895).

The corrosion potential of the S235 steel (Ecorr), in present investigation was observed to be −0.0113 V. The anodic (ba) and cathodic (bc) Tafel slopes were 0.074 and 0.468 respectively. The polarization resistance (Rp) was 4328.The corrosion current (Icorr) was calculated based on equation (1) as per ASTM G59-97 [5][6], and was found to be 6.39 µA, which corresponds to a corrosion current density (icorr) of 12.73 μ A/cm^2. It is to be noted that in Figure 8., since the current density is plotted in logarithmic scale to the base 10, the absolute value of i_{corr} is obtained from the antilog of the ordinate of the point of intersection of cathodic and anodic slopes. A similar order of density of corrosion currents has been reported in literature for mild steel and martensic steel samples, respectively [7], [8]. Additionally, the corrosion current density for all samples and the mean of the first five samples are tabulated in Table 3. The value of sample number 6 was not taken into account for calculation of the average due to accidental disturbances during the Tafel experiment.

$$icorr = \frac{ba\ bc}{2.303(ba+bc)Rp} \qquad (1)$$

where:

ba = slope of the anodic Tafel reaction, when plotted on base 10 logarithmic paper in V/decade,
bc = slope of the cathodic Tafel reaction when plotted on base 10 logarithmic paper in V/decade,

3.2 Prediction of mass loss

The magnitude of the corrosion rate is expected to have a significant effect on tensile strength, deformational behavior, ductility, bond strength and mode of failure of the bi-material adhesive joint in real life application. Consequently, the degree of corrosion is considered to be a key parameter for predicting the useful service life of such adhesive joint. It is possible, with varying degrees of accuracy, to calculate the amount of steel dissolved and oxidized (rust). The corrosion penetration rate (CPR) for S235 steel was estimated at 0.115 g/cm^2/year and 0.143 mm/year by using Faraday's [1] equation (2) and ASTM G102-89 [9] equation (3) respectively. These equations can also help to estimate the rate of the reaction.

$$r(in\ mpy) = 0.129\frac{\mathrm{a}i_{corr}}{\mathrm{nD}} \text{ and } r\left(\frac{g}{cm2}\right) = r(in\ mpy)0.00254\mathrm{D} \quad (2)$$

$$r\left(\frac{mm}{year}\right) = K_1\frac{i_{corr}}{\mathrm{D}}EW \quad (3)$$

where, a= atomic weight of corroding metal (gram), n = electrons transferred in oxidation reaction (mole) / number of electrons (n = 2 for Fe^{2+}), i_{corr} = corrosion current density of electrode material (i_{corr} = 12.60 ampere/cm^2), D = density of the steel, 0.129= Conversion constant, EW= Equivalent Weight (gram), r = Corrosion rate (g/cm2 or mm/year), K_1 = 3.27 x 10 $^{-3}$ (mm g/μA cm yr), mpy = mils per year.

4. Electrical conductivity

In the preliminary electrochemical corrosion experiments, the same electrolyte solution has been used in TACM, whereas in SACM a fresh salt solution was prepared for each test. According to fundamental electrochemistry, the chemical stability of salt water is disturbed by the increasing rate of soluble corrosion products during the electrochemical corrosion process and consequently the electrical conductivity of the electrolyte solution deteriorates with increasing process time. Also, Arrhenius' theory states that the ionic conductivity of an electrolyte solution is determined by its electrolyte ions [10].

(a) (b)

Figure 9 The state of electrolyte solution at the start (a) and after 96 hours (b) during electrochemical corrosion. A- Adherend connection.

These observations encouraged the study on the electrical conductivity of artificial seawater when it acts as electrolyte solution in the electrochemical corrosion processes. For that purpose, a double lap adhesive joint was fabricated. Direct contact between the steel substrates was not achieved in the first batch of DLAJ production, therefore the connection was completed using an additional electrical wire, which can be seen as 'A' in Figure 9. When a pre-determined electro-processing time interval of 24 hours was obtained, the sample was retrieved and weighed (without cleaning corrosion product) followed by drying. In order to ensure complete drying of the sample and to protect the fragile residual corrosion on the sample, lower speed of hot air from the dryer was maintained for 15 minutes. The sample was reinserted into the electrolyte solution and the electrochemical process was continued till

120 hours. It was observed that the connection was lost after 96 hours due to wearing off of copper wires with respect to increasing time of electrochemical corrosion.

A similar process as described for the preliminary corrosion tests has been applied to evaluate the effect of electrochemical corrosion on double lap joints. In this test, a current of 1.2 A (detail calculations can be found in the attached excel sheet) was applied based on Faraday calculations. Based on Faraday's law, the specimen requires up to 5 days of experimentation to achieve a mass loss which corresponds to a service exposure time of 20 years. The changing state of electrolyte solution due to the dissolution of ionic solids can be seen in Figure 9 (a) and (b).
Figure 14 shows the predicted (theoretical) and experimentally measured mass loss of the sample up to 96 hours of electrochemical corrosion (at that time the anode connection was lost) . The results suggest that the percentage mass loss of the steel strips gradually decreased with an increasing reaction time. The mass loss during the first 72 hours was in line with the expected values, but a significant difference between measurement and prediction has been observed at a period of 96 hours. The predicted (theoretical) and experimental mass losses of DLAJ after 24, 48, 72, and 96 hours are also tabulated in Table 4. Anodic dissolution of iron is a complex process that depends on many factors such as the presence of chloride ions, pH, possible dissolution of passivated oxides, electrolyte convection, the electrode potential etc. However the electrical conductivity of electrolyte solution one of major factor, which can be influenced on chemical activity in corrosion process. Therefore, It can be hypothesized that the result for 96 hours of exposure was influenced by the deterioration of the electrical conductivity of the electrolyte solution (because of the linear relation between conductivity and NaCl concentration [10]).

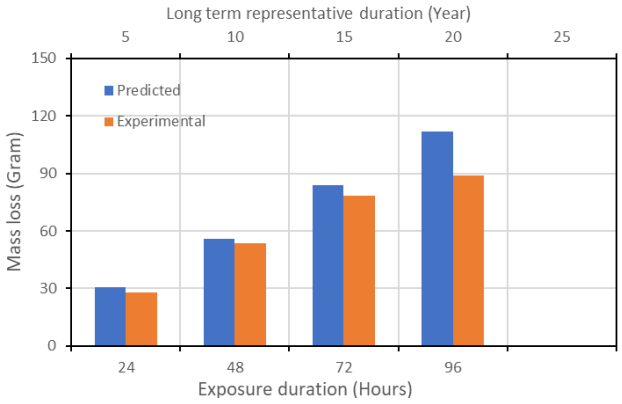

Figure 10 Predicted versus experimental mass loss at different durations of exposure.

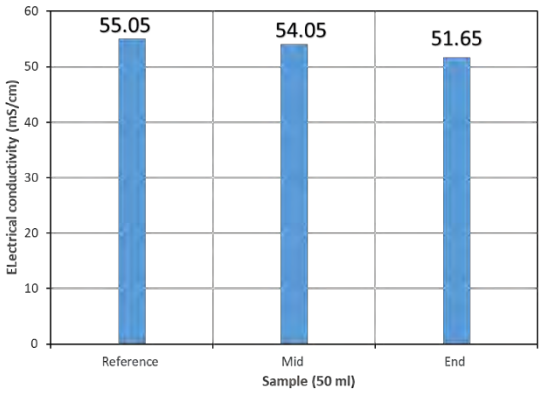

Figure 11 Ageing effect on electrical conductivity of artificial seawater.

Table 4 Summary of the test results

Representative service life (Years)	Exposure duration (Hours)	Theoretical (Predicted) Mass loss (Grammes)	Experimental mass loss (Grams)	Difference (Grams)
05	24	30.5	28.0	2.5
10	48	56.0	53.6	2.4
15	72	84.0	78.5	5.5
20	96	112.0	89.1	22.9

The increasing fraction of soluble corrosion products perturbed the concentration of NaCl, and accumulated rust over the steel leads to a slowdown of the migration of ions and rate of corrosion during

electrochemical corrosion[11] [12] [13]. In order to validate literature observations and own experimental results, the electrical conductivity of the electrolyte solution (artificial seawater) was measured using Orion star A212 conductivity meter (range of 0.001µS to 3000 mS with an accuracy of 0.5% of reading ±1 digit for values > 3 µS, 0.5% of reading ±0.01 µS for values ≤ 3 µS). Two samples of 50 ml have been taken out for measurement of electrical conductivity and have been compared with reference (pure) artificial seawater. Figure 11 shows that electrical conductivity of artificial sea water indeed decreases with increasing reaction time, which confirms our hypothesis. The magnitude of electrical conductivity has decreased significantly from 55.05 ms/cm to 51.65 ms/cm.

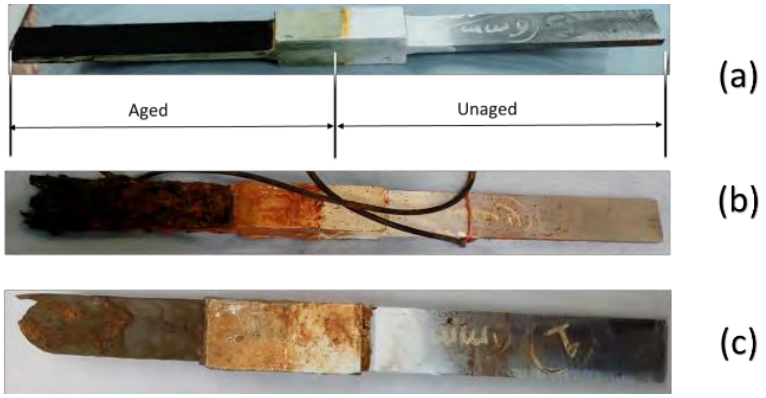

Figure 12 The state of specimens after (a) 24, (b) 76 and (c) 96 hours of electrochemical exposure.

Notwithstanding the objective of this experiment was to study the electrical conductivity of the electrolyte solution, the effect of electrochemical corrosion effect can be seen on the exposed part of the specimen in Figure 12. No significant mass loss was observed at the steel adhesive interface.

5. Effect of electrochemical corrosion on painted sample

In order to gain a deeper understanding and to see the influence of electrochemical corrosion on painted steel specimens, the following experimental program was planned with a single anode electrochemical cell method. Steel samples measuring 300x25x6 mm^3 were used; the front and back surfaces (150 mm x 25 mm) of sample 1 and the bottom surface (25mm x 6mm) of sample 2 were exposed to electrochemical corrosion. The remaining parts of both specimens were protected by applying an anti-corrosive paint (see Figure 14). During the experiment, sample 2 was raised 20 mm from the bottom of the container so that corrosion could occur on the unprotected region of steel part, whilst sample 1 rested on the bottom till the end of test, as shown in Figure 13,.

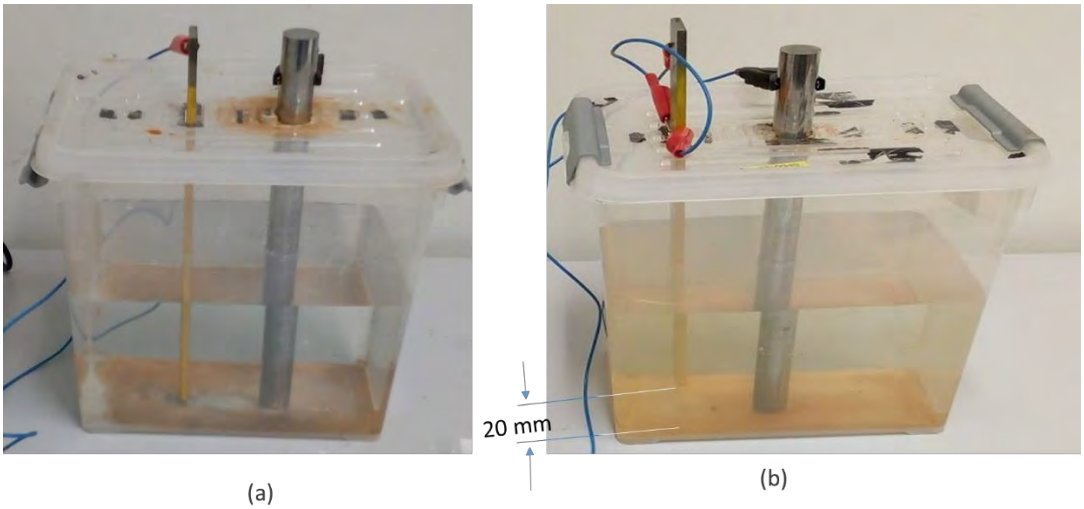

Figure 13 Laboratory view of basic electrochemical cells for (a) sample 1 and (b) sample 2.

The mass of both specimens was measured in a controlled environment using a weighing machine with an accuracy of 0.01 gram. The actual appearance of the steel specimens and boundary conditions of paint can be seen in Figure 14. Electrical current intensities of 1.20 and 3.62 A were chosen based on Faraday's calculations to achieve considerable mass losses for sample 1 in 24h (representing 5 years of service life) and sample 2 in 1h (representing 25 years of service life) respectively. Eventually, the unprotected parts of both specimens were subjected to electrochemical corrosion, followed by retrieving and weighing both samples as discussed in section 4.

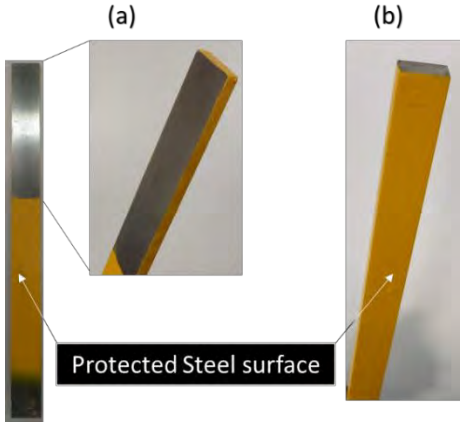

Figure 14 The boundary conditions of paints on control samples: (a) sample 1 (b) sample 2

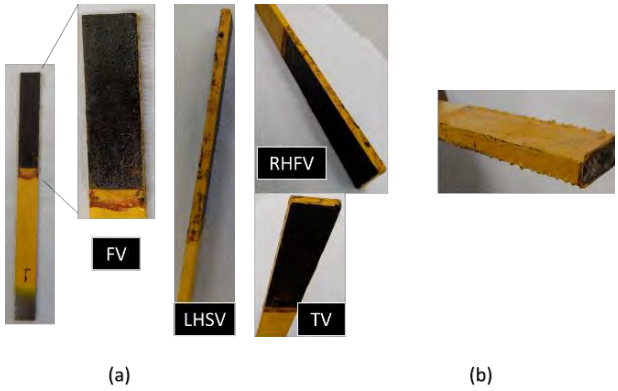

Figure 15 Effect of electrochemical corrosion on (a) sample 1 (b) sample 2.

Figure 15 shows the state of both specimens after the electrochemical corrosion. The immersed part of specimens appeared dark brown (rust) due to the formation of hydrated ferric oxide Fe(OH)2 and exchange of electrons between anode and cathode in the electrolyte [14]. The surface of the rusty steel was asymmetrical, and the edges of the specimens exhibited greater corrosion damage than other areas which looks like a phenomenon of filiform corrosion [15].

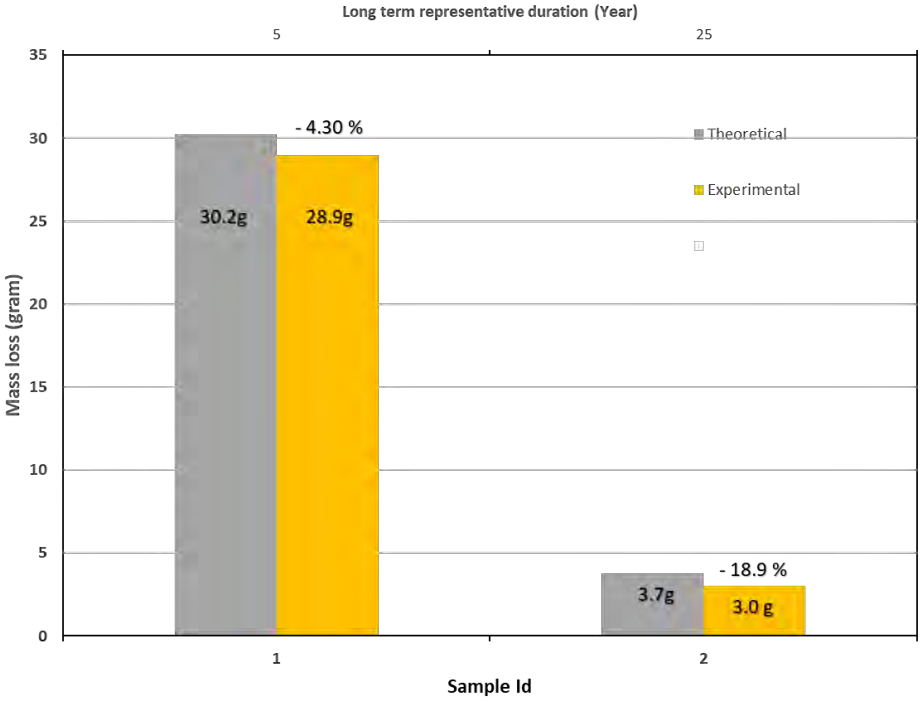

Figure 16 Comparison of theoretical versus experimentally measured mass losses for sample 1 and 2.

The barrier effect of the coating against reaction agents is at its lowest in areas with reduced coating thickness, and the presence of corrosion is at its greatest. Likewise, the effect of electrochemical

corrosion can also be seen at the edges in the form of thin filaments for both specimens. The presence of surface defects in the coating is closely related to the inherent brittleness of the paint coating and its application procedure. This effect can be minimized if the sharp edges of the sample are coated correctly. The approximate average width of filaments for coated steel was reported to be 0.2 mm [16].

The experimentally measured mass loss values were compared with the predicted (theoretical) values (based on Faraday's law) for samples 1 and 2. These are shown in Figure 16., including percentage mass loss errors (i.e. 4.30 % and 18.9 %). The experimentally measured value for sample 1 is much closer to the predicted values as compared to sample 2. It is, however, difficult to justify the mass loss result of sample 1 compared to sample 2 because of several influential factors including diffusion, temperature, conductivity, type of ions, pH value and electrochemical potential influence the rate of corrosion. However, on the basis of our observations, it can be concluded that a higher current intensity causes a higher rate of corrosion but the downward direction of the exposed area of sample 2 might have disturbed and slowed down the reaction activity in the electrochemical process.

In order to quantify the effect of electrochemical corrosion, the corroded surface was cleared using a hand grinder to obtain an acceptable surface finish for measuring the remaining thickness of sample 1. The final appearance of the sample is shown in Figure 17. The thickness at the centre has decreased from 5.9 to 4.7 mm, while 3.6 mm and 3.2 mm were noted on the left and right edges respectively, which confirm the effect of electrochemical corrosion at the interface barrier of paint film and steel surface. The coating of becomes brittle due to strains developed by corrosion products, which leads to cracks and a broken layer of paint [15], which can be clearly seen in Figure 17 (b).

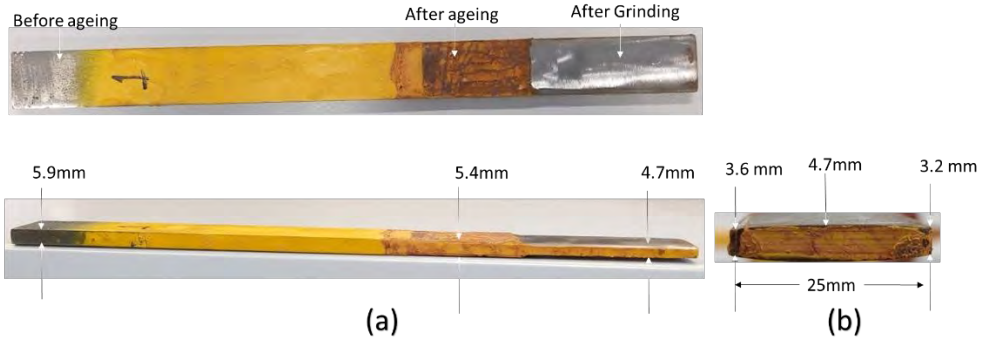

Figure 17 Effect of electrochemical corrosion on (a) surface and (b) cross section of sample-2.

6. Ageing of double lap adhesive joint specimens

This experimental program was carried out using the electrochemical corrosion method explained in section 1. For that purpose, four double lap joints with 6 mm adhesive thickness and 60 mm overlap length were fabricated using a mould. These joints were cured at room temperature for at least 24 hours and then their mass was measured using a weighing machine with an accuracy of 0.01 g. The geometry and dimensions of the double lap joint are shown in Figure 18. The periphery of the adhesive including the edges of the adherend were protected by applying an anti-corrosive paint, so that corrosion is possible on the steel surface and at the interface of the adhesive-steel region. The partially coated specimens before ageing treatment are shown in Figure 19a. The goal is to investigate the effect of single and triple anode electrochemical corrosion methods on the evolution of the unprotected region of double lap adhesive joints.

The electrochemical cells are shown in Figure 20. Electrical current intensities of 1.38 and 4.15 amperes were chosen based on Faraday's calculation to achieve similar mass losses in both SACM and TACM electrochemical corrosion setups in a period of 24 h, which represents a 5-year service life of the sample under saline environments.

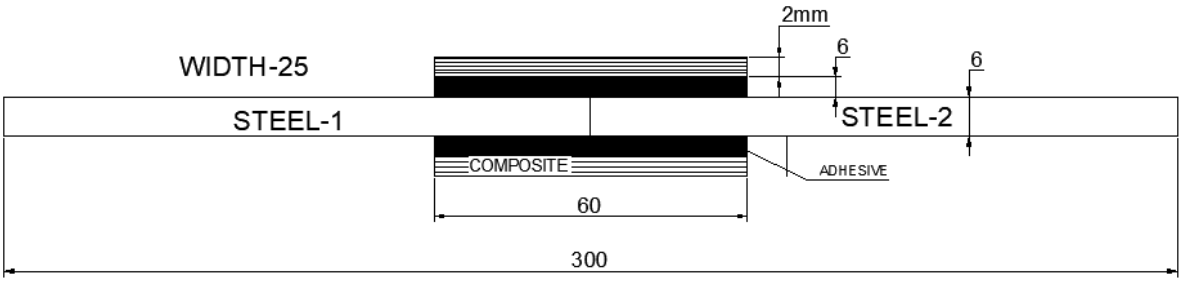

Figure 18 Schematic diagram of a double lap adhesive joint.

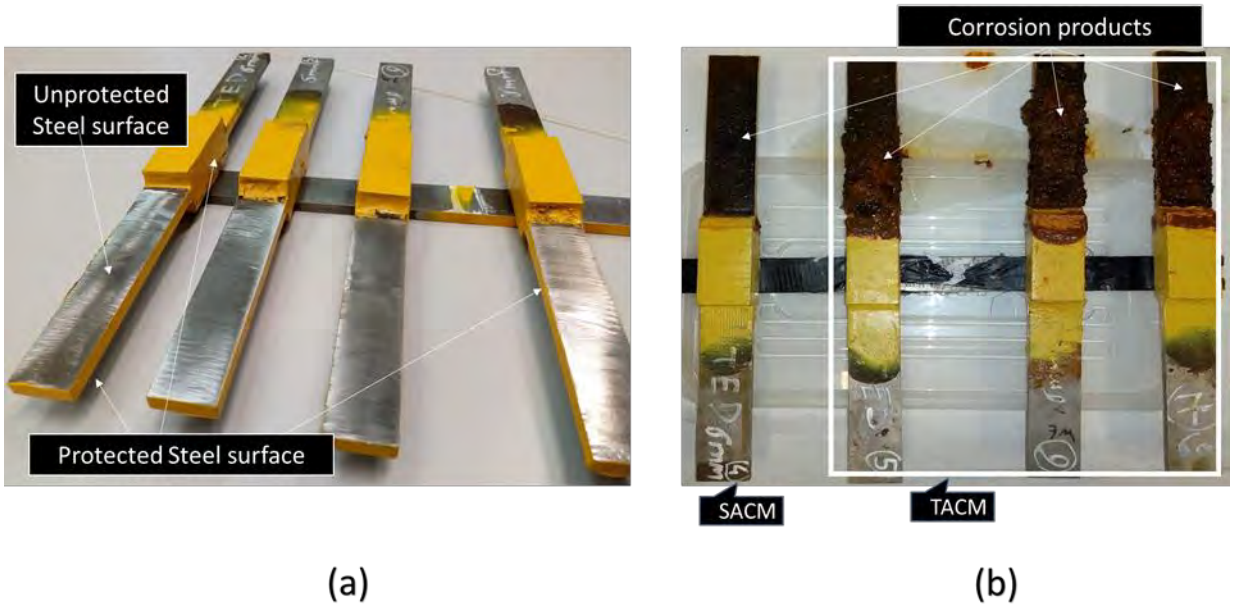

Figure 19 Effect of electrochemical corrosion on specimens before ageing (a) and after ageing (b).

Half of the bond length and the area below the joint were subjected to electrochemical corrosion (Figure 20). When the pre-determined electro-processing time was obtained, the process was stopped. All samples were retrieved, weighed and aged specimen were cleaned based on ASTM G1-03 [17], as discussed in previous section.

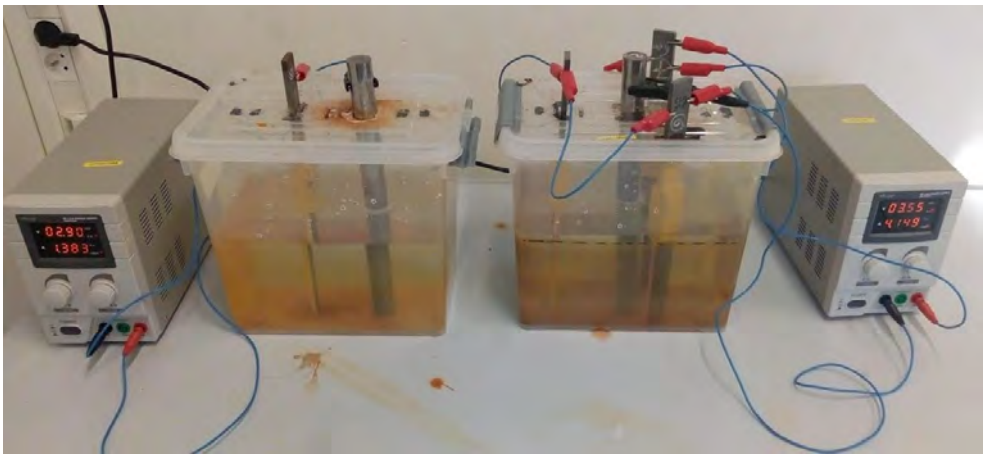

Figure 20 Laboratory view of basic electrochemical cells ((a) SACM, (b) TACM).

Following the cleaning process, the effect of both electrochemical corrosion processes were measured in terms of degraded thickness over the control thickness of DLAJ sample. The thicknesses along the

center of the sample were almost identical for both cases, while significant differences in steel thickness were recorded at the edges of the samples (Figure 22). The rectangular cross-section of the DLAJ turns into a convex cross-section due to the effect of filiform corrosion, as confirmed and discussed in section 6.2. The contact area between the grips of a tensile testing machine and the adherend would be reduced due to this convex shape which could cause slippage and misalignment during a tensile test.

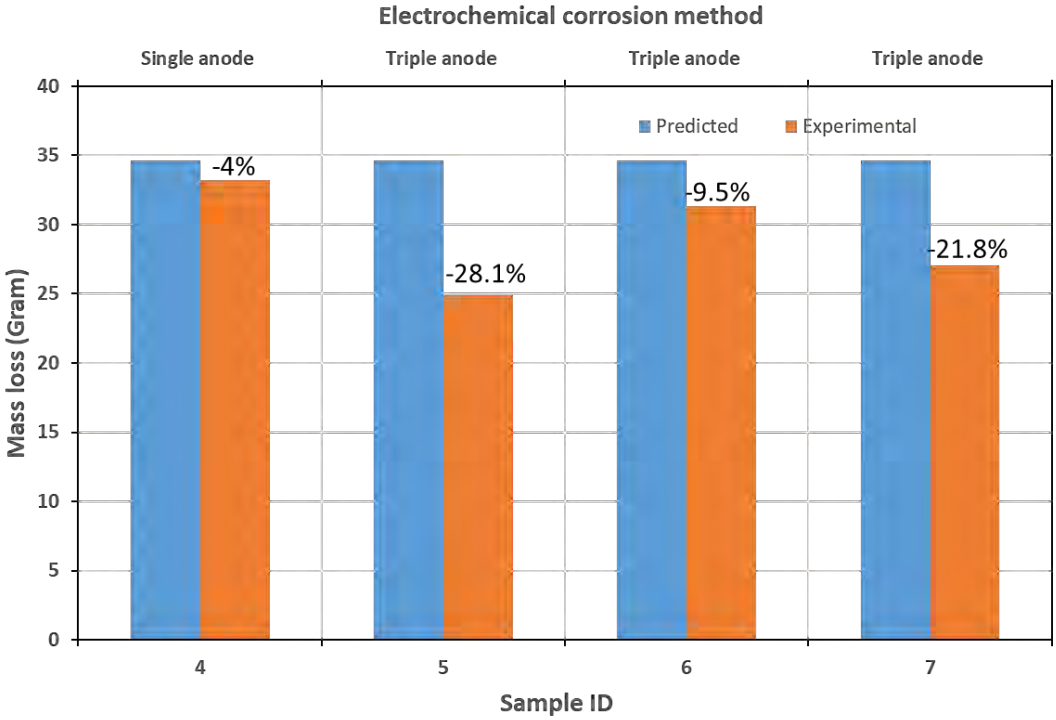

Figure 21 Comparison of predicted versus experimentally measured mass losses for a representative service life of 5 years reached in 24 hours.

Table 5 Summary of the test results for simulated 5 years of exposure to a saline environment.

Sample ID	Duration of exposure (Hours)	Type of corrosion method	Current intensity (Amperes)	Theoretical (predicted) mass loss (Grams)	Experimental mass loss (Grams)	Difference in mass loss (Grams)
04	24	SACM	1.38	34.6	33.2	1.42
05		TACM	4.14	34.6	24.9	9.73
06				34.6	31.3	3.31
07				34.6	27.1	7.55

Figure 19 shows the state of DLAJ specimens before and after the electrochemical corrosion. The immersed part of the specimens appeared as dark brown (rust) due to the formation of hydrated ferric oxide Fe(OH)2 and exchange of electrons between anode and cathode in electrolyte [14]. The surface of the rusty steel was asymmetrical, and the edges of the specimens exhibited greater corrosion damage than other areas due to the phenomenon of filiform corrosion [15]. Figure 21 shows the experimentally measured loss values as compared with the predicted values (based on Faraday's law). As discussed higher, the rate of corrosion slows down due to the increasing percentage of dissolved corrosion products with respect to increasing the reaction time in electrochemical corrosion. The released rate of dissolving corrosion products from three anodes in TACM was higher than for the single anode in SACM. Therefore, experimentally measured loss values with SACM are closer to the predicted mass loss values

as compared to TACM. A mass loss difference (between prediction and experiment) of 4% was observed for the sample tested with SACM, while differences from 9.5 to 28.1% were recorded for the specimens tested in TACM. The magnitude of mass losses for each DLAJ and both electrochemical process are tabulated in Table 5.

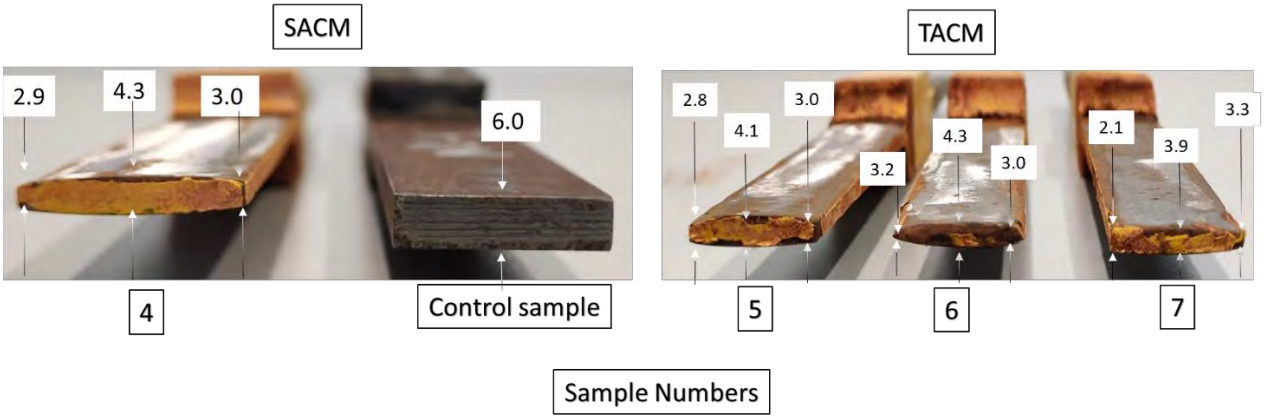

Figure 22 Effect of SACM and TACM on the thickness of DLAJ specimens over the control sample. (All dimensions are in mm)

7. Alignment of the specimen and filiform corrosion

In order to see the influence of electrochemical corrosion on the failure mode and strength of DLAJ sample, tensile tests will need to be conducted. During such test, perfect alignment is required between two adherends, and the geometry and dimensions of the specimen grip area should be the same before and after the electrochemical corrosion.

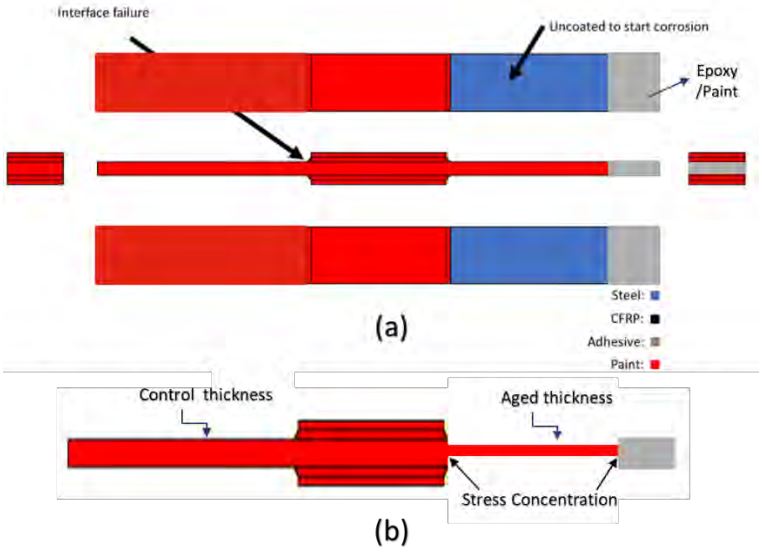

Figure 23 A schematic of double lap joint: (a) Epoxy + paint coated grip area; (b) stress concentration due to material loss.

For this purpose, the left side of the sample and the grip area at the right side of the sample were coated (Figure 23(a)). After electrochemical corrosion, this coating condition can cause stress concentrations near the grip area and the steel-adhesive interface (Figure 23(b)). Two dummy samples (anodes) were aged whilst positioned in two different orientations with respect to the cathode, Figure 24. The goal is to evaluate the influence of the specimen orientation on corrosion in terms of mass loss at each side of the adherend, including the grip area. Based hereon, the optimal approach can be chosen for future tensile experiments. In the conducted electrochemical corrosion experiment, the same process parameters (i.e time of reaction and current intensity) as mentioned in the previous section have been used.

Figure 24 Orientation of anode:(a) parallel, (b) perpendicular.

Figure 25 Top view of electrochemical cells setup.

After the predefined ageing time, the corrosion process was stopped and samples were cleaned using acetone and (soft) wire brush. This procedure was followed in order to only remove corrosion products from the specimen and to protect the original surface of the specimen. Following the remaining thickness of the cleaned steel part was compared with the non-corroded part of the specimen.

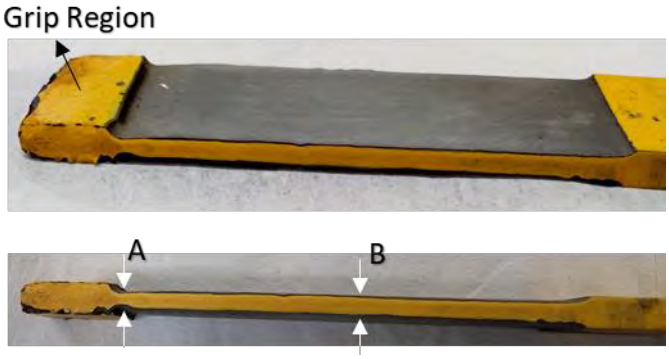

Figure 26 Effect of electrochemical corrosion on thickness at the interaction of grip region (A) and corroded area of the specimen (B). Thickness is measured along the edge of the specimens.

No significant difference could be observed between the two samples. Likewise, there is no noticeable change in cross-section at the grip region of the specimen. However, more significant material loss was found at location 'A' (i.e intersection of the grip area and the corroded surface of the specimen) as compared to location 'B' (i.e along the length of side edge the specimen) (see Figure 26).The reduction in thickness at point A was about 0.94mm for the perpendicular and 0.98mm for the parallel orientation of the anode in the electrochemical corrosion setup. In contrast, 0.59 mm thickness reduction was measured at point B. The thickness measurement of the aged part of the specimen will be performed more accurately in the future with a 3D scanning device (current measurements were performed with a micrometre). Since no literature is available about the perpendicular orientation of anode in the electrochemical process, and several researchers support the parallel orientation method, it will also be selected for our future corrosion experiments.

8. Tensile test and representative service life

Three different overlap lengths (60mm, 80mm and 100mm) and three different adhesive thicknesses (2mm, 4mm and 6mm) were defined to establish an experimental matrix to study the influence of accelerated ageing on failure mode and ultimate strength of bi-material adhesive joints. In total 27*3 specimens are being made. Of each configuration, three specimens are produced for three different corrosion experiments (i.e. replication of 3, 4 and 5 years of exposure to a corrosive environment). Due to the Covid-19 measures, the ageing and strength tests could not yet be started.

9. Conclusion

This document presents an experimental study using dummy steel specimens and bi-material adhesive joints subjected to accelerated corrosion to investigate various experimental parameters. The following topics have been discussed: single anode versus triple anode electrochemical corrosion methods, prediction of mass loss and rate of corrosion, electrical conductivity of electrolyte solution, the effect of filiform corrosion on painted samples and suitable coating boundary conditions. Based on the observations and the results of the experimental program, the following conclusions are drawn:

- Single anode electrochemical corrosion method is more efficient and more accurate than the three anode electrochemical corrosion method.
- The deterioration of steel samples (adherends of double lap joints) subjected to accelerated corrosion conditions can be predicted using Faraday's equation and Tafel experiments. The predicted mass loss based on Faraday's equation has been validated with experimental mass loss.
- The electrical conductivity of the electrolyte solution decreases with an increasing rate of corrosion products and reaction time.
- The effect of filiform corrosion on the coated part and grip area of the specimen can be reduced by using good quality anti-corrosive paint with appropriate boundary conditions.
- It is possible to replicate 5 years of exposure on a joint to a saline environment in 24 hours of accelerated corrosion.

10. References

[1] Denny A jones, "Principles and prevention of corrosion." Prentics Hall, Upper Saddle River, NJ 07458, 1996.

[2] T. A. El Maaddawy and K. A. Soudki, "Effectiveness of impressed current technique to simulate corrosion of steel reinforcement in concrete," *J. Mater. Civ. Eng.*, vol. 15, no. 1, pp. 41–47, 2003.

[3] J. Bonacci, M. Thomas, N. Hearn, C. Lee, and M. Maalej, "Laboratory simulation of corrosion in reinforced concrete and repair with CFRP wraps," in *Proceedings of the Annual Conference of CSCE*, 1998, pp. 653–662.

[4] ASTM D1141, "Standard Practice for the Preparation of Substitute Ocean Water," *ASTM Int.*, vol. 98, no. Reapproved 2013, pp. 1–3, 2013.

[5] ASTM G-59-97, "Standard Test Method for Conducting Potentiodynamic Polarization Resistance Measurements 1," *Astm*, vol. 97, no. Reapproved 2009, pp. 1–4, 2003.

[6] P. R. Instrumentation, "Linear Polarization Resistance and Corrosion Rate," *Https://Www.Pineresearch.Com/Shop/Documentation-Index/*, vol. 10086, pp. 1–14, 2016.

[7] X. Y. Wang and D. Y. Li, "Application of an electrochemical scratch technique to evaluate contributions of mechanical and electrochemical attacks to corrosive wear of materials," *Wear*, vol. 259, no. 7–12, pp. 1490–1496, 2005.

[8] K. Pondicherry, J. Vancoillie, J. De Pauw, J. Sukumaran, D. Fauconnier, and P. De Baets, "Design and development of a novel electrochemical abrasion-corrosion tester," *Tribol. Int.*, vol. 131, pp. 652–660, 2019.

[9] Astm G 102, "Standard Practice for Calculation of Corrosion Rates and Related Information," *Astm G 102*, vol. 89, no. Reapproved, pp. 1–7, 1999.

[10] C. S. Widodo, H. Sela, and D. R. Santosa, "The effect of NaCl concentration on the ionic NaCl solutions electrical impedance value using electrochemical impedance spectroscopy methods," *AIP Conf. Proc.*, vol. 2021, no. 2018, 2018.

[11] NACE International, "Techniques for Monitoring Corrosion and Related Parameters in Field Applications," *NACE Int. Publ. 3T199*, no. 24203, 1999.

[12] K. R. Trethewey and J. Chamberlain, *Corrosion for students of science and engineering*. 1988.

[13] Y. J. Kim, I. Bumadian, and J. S. Park, "Galvanic current influencing interface deterioration of CFRP bonded to a steel substrate," *J. Mater. Civ. Eng.*, vol. 28, no. 2, pp. 1–10, 2016.

[14] R. A. Buchanan and E. E. Stansbury, *Electrochemical corrosion*. 2005.

[15] A. Bautista, "Filiform corrosion in polymer-coated metals," *Prog. Org. Coatings*, vol. 28, no. 1, pp. 49–58, 1996.

[16] T. A. Adler, D. Aylor, and A. Bray, *Corrosion: Fundamentals, Testing, and Protection*. ASM International, 2003.

[17] ASTM G1-90, "Standard Practice for Preparing, Cleaning, and Evaluation Corrosion Test Specimens," *Astm G1-90*, no. G1-90, p. 8, 1999.